

EVALUATION OF ACCURACY AND RESOLUTION OF THE ELECTRON BEAM PROFILE SCANNER AT THE FERMILAB MAIN INJECTOR*

M. W. Mwaniki^{†,1}, P. Snopok, Illinois Institute of Technology, Chicago, USA
 R. Thurman-Keup, R. Ainsworth, Fermi National Accelerator laboratory, Batavia, USA
¹also at Fermi National Accelerator laboratory, Batavia, USA

Abstract

The objective of this work is to assess the accuracy of measurements made by the Electron Beam Profile Scanner (EBPS), which captures the trajectory of an electron beam with and without a proton beam present. The proton beam induces deflection in the electron beam, which is influenced by proton charges. For high-resolution images, the probe beam needs to be of high intensity, small diameter, and small divergence, evaluated using a phosphor screen and an optical transition radiation (OTR) screen. The capabilities of the Kimball Physics electron gun (eGun) will be considered for accuracy. Additionally, the Zemax software will be utilized to characterize the optical elements.

INTRODUCTION

Understanding the accuracy and resolution of measurement devices is important in order to obtain useful data during measurements. This work focuses on the Electron Beam Profile Scanner (EBPS), a non-invasive measurement tool that determines the transverse beam size of a proton beam using an electron probe beam [1].

Electron Beam Profile Scanner

The EBPS consists of a triode electron gun (eGun) [2], electrostatic deflectors, an intersection space with the proton beam pipe, an optical transition radiation (OTR) mirror that is only inserted in the absence of the proton beam for measuring the size of the electron beam, a $Y_2SiO_5:Ce^{3+}$ phosphor screen [3] that records the electron beam trajectory endpoints and an imaging system consisting of mirrors, lenses, an image intensifier, and a charge injection device (CID) camera that records images of the phosphor and OTR screen during measurements. An exhaustive composition of the EBPS system has been presented before [4], and its measurement techniques have also been discussed [5].

An evaluation of the accuracy and resolution of the EBPS will be conducted by characterizing eGun and the optical components of the EBPS imaging system. The ultimate goal is to achieve EBPS measurements with a resolution of ± 0.2 mm, leading to the capability of single bunch measurements.

* Work supported by Fermi Forward Discovery Group, LLC manages and operates the Fermi National Accelerator Laboratory pursuant to Contract number 89243024CSC000002 with the USAs Department of Energy.
[†] mmwaniki@hawk.illinoistech.edu

eGUN CHARACTERIZATION

The eGun is the source for the electron probe beam. In order to have improved precision and accuracy, the probe beam is required to be intense with a small divergence and a small diameter relative to the proton beam [6]. Characterizing the eGun is essential to ensure the probe beam has these qualities.

Beam Intensity of the eGun

Beam intensity refers to the amount of electrons emitted from the eGun. Low intensities may allow the protons to interfere with the trajectories of the electrons, while excessively high intensities can damage to the measurement screens. The electron beam intensity is currently regulated by the eGun's cathode and grid voltages and it is measured by collecting the electrons emitted with a Faraday cup that surrounds the phosphor screen as the two voltages are scanned.

The goal was to achieve an electron beam intensity of about 500 μA during measurements. The results are summarized in Fig. 1. The results indicated that 53.9 μA was

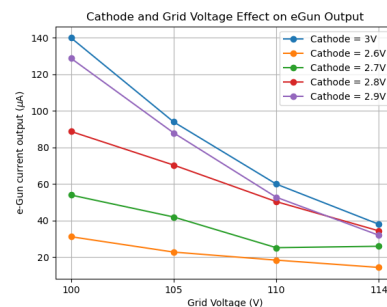


Figure 1: Cathode and grid voltage scan effect on beam intensity from the eGun.

sufficient and higher intensities were unnecessary. Consequently, the ideal setpoint for the cathode voltage was found to be 2.7 V and 100 V for the grid voltage.

Diameter of the Electron Beam from the eGun

The diameter of the electron beam refers to the spot size of the beam, which directly influences the resolution of measurements, much like how wire size and spacing affect precision in a multi-wire. The spot size of the electron beam is controlled by adjusting the eGun's solenoid current and is measured in two ways: 1) using the OTR screen at the proton interaction region (PIR) and 2) using a phosphor screen located below the PIR.

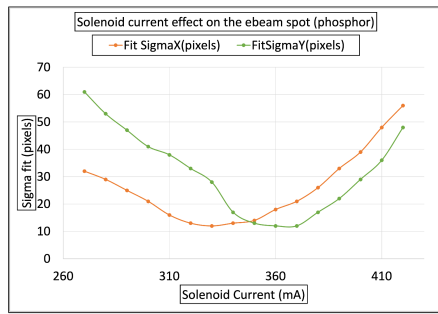


Figure 2: Solenoid scan effect on the electron beam diameter at the phosphor screen.

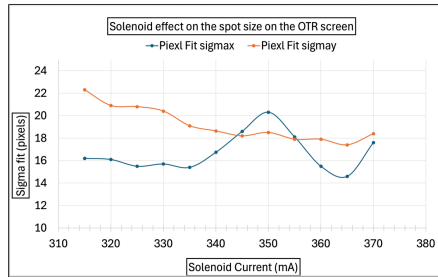


Figure 3: Solenoid scan effect on the electron beam diameter at the PIR.

The primary objective of the spot size measurements was to minimize the transverse diameter of the electron beam. The solenoid scan revealed a minimum beam spot size of 11 px (~ 1.21 mm) at the phosphor screen and 18 px (~ 1.98 mm) at the PIR, as shown in Figs. 2 and 3. These measurements correspond to the intersection point of the “SigmaX” and “SigmaY” traces, indicating a nearly circular beam. Consequently, the optimal solenoid current was selected to be 345 mA, which closely aligns with the simulation result of 339 mA obtained from the solenoid and the drift space transfer matrices.

The initial scan images were out of focus due to lens misalignment. After correcting the lens position, the minimum spot size remained at the same solenoid setting, and were then used for divergence calculations.

Divergence of the Electron Beam

Beam divergence is a measure of how much a beam spreads out as it travels away from its source. Divergence is calculated from the obtained spot sizes at the PIR and at the phosphor screen which are separated by ~ 200 mm. Figure 4 shows the minimum spot sizes of 0.605 mm at the PIR (OTR) and 1.32 mm at the phosphor, with a measured divergence of 3.575 mrad. This divergence angle will be utilized to balance the inverse relationship between PIR and phosphor spot sizes to optimize both profile precision.

CHARACTERIZING OPTICAL ELEMENTS

During measurements, both the OTR and phosphor screens are imaged in two separate optical paths, before getting to the image intensifier and the camera as seen in Fig. 5.

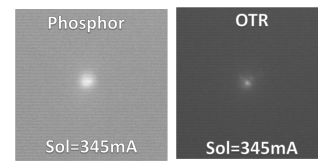


Figure 4: Electron beam diameters at 345 mA solenoid: OTR screen 0.605 mm and phosphor screen 1.32 mm.

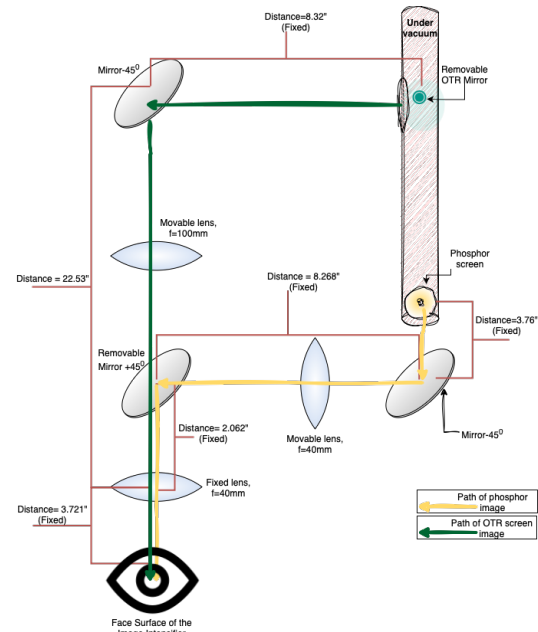


Figure 5: A representation of the optical elements layout for phosphor and OTR (PIR) screens image collection.

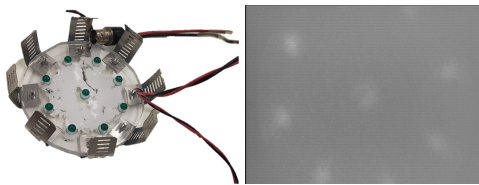
The optical path indicated in green is used to image the OTR screen which is inserted into the proton interaction region (PIR) in the absence of protons to measure the diameter of the electron beam. The OTR light is bent 90° downwards by a mirror and passes through a movable lens with a focal length of 100 mm, through a fixed lens with a focal length of 40 mm, and finally reaches the image intensifier and camera.

The optical path indicated in orange is used for imaging the phosphor screen after removing the OTR screen to allow electrons to reach the phosphor screen and measure proton beam size. The light is bent 90° to the left by a mirror and passes through a movable lens with a focal length of 40 mm, then is bent 90° downwards through the fixed lens, image intensifier and camera that are shared by both configurations.

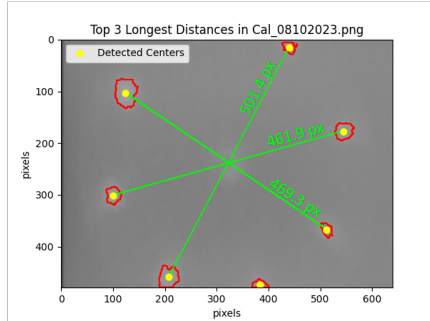
In this section, the calibration of the images to convert pixels to physical units, the optical lens alignment, and detection accuracy using python image processing [7, 8] will be systematically evaluated.

Pixel-to-Millimeter Calibration

In order to determine the a pixel-to-millimeter conversion factor, a calibration device was designed using Plexiglass and fitted with LED bulbs, each with a radius of 3 mm. These bulbs were positioned 50.8 mm apart from one another in a radial arrangement. The device was then positioned at



(a) Device for pixel calibration and its raw image



(b) Distances seen in the image observed by the camera.

Figure 6: Image calibration using an LED device as observed by the camera.

the location of the phosphor screen and captured using the camera seen in Fig. 6a.

A calibration factor was calculated from values indicated in Fig. 6b to be 0.11 ± 0.004 mm/px. The uncertainty arises from the standard deviation across the three measurements and will inform conversion of image-based dimensions to physical units.

Spot Detection Accuracy Using Python

The image shown in Fig. 6b is used to evaluate the accuracy of spot edge and center detection performed by Python in identifying spots on the phosphor screen.

By comparing the observed spot radii with the known LED radius, an estimated pixel-to-millimeter conversion of 31.375 ± 8.03 px ($\sim 0.05 \pm 0.02$ mm/px) was obtained, which is approximately half of the expected value. This discrepancy, along with the large uncertainty, suggests that the image may be out of focus. Future efforts will include refocusing and re-imaging to verify the image processing code on diameter-based calibration and yielding consistent results with center detection.

Optical Lens Alignment

Initial images collected during measurements were noticeably out of focus, prompting an optimization of the movable lens position to reduce the focal spot size from the OTR screen. Simulations using Zemax [9] used thick lens approximations to refine the distances between the OTR and phosphor screens, lenses, and image intensifier for improved optical accuracy. The simulations revealed a halo around the central spot, which was observed during measurements (see Fig. 7 left). Zemax suggested reducing the distance between the fixed lens and the image intensifier. However, this modification led to unexpected secondary spots on the image (see Fig. 7 right). These multiple beam spots suggest potential

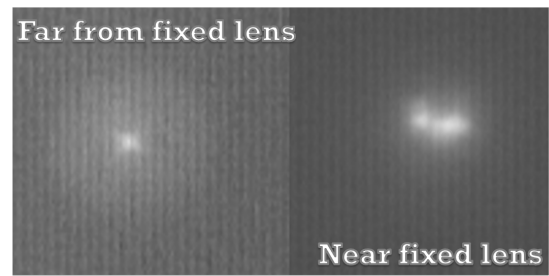


Figure 7: Raw images of OTR imaging from varying positions of the movable lens. Far from the fixed lens (left), near the fixed lens (right).

optical aberrations or stray ray paths. To evaluate diffraction effects, thin lens approximations were applied based on the lens aperture, detection wavelength, and source distance [10]. The calculations indicated that diffraction is not the primary issue, as the system operates within its diffraction limit. The exact cause of the artifacts remains unclear. Further investigation will include polarization-dependent analysis of the OTR light using Physical Optical Propagation (POP) in Zemax and ensuring that the lenses are not tilted post-adjustment.

DISCUSSION

Evaluating the accuracy and resolution of the EBPS is essential for precise beam profile measurements. The error margins in the profile measurements will result from factors determined during the eGun characterization, statistical uncertainties, and the characterization of the system's optical elements. The eGun is characterized by high intensity, small diameter and minimum divergence of the electron beam. The intensity determined to be $53 \mu\text{A}$, and the smallest spot sizes revealed a divergence of 3.575 mrad. This divergence angle will be used to optimize spot sizes at PIR and phosphor screen to prevent loss of resolution.

Future work will concentrate on addressing additional sources of error. In the beam intensity analysis, further investigation will explore the relationship between cathode temperature, voltage, and output to assess their influence on eGun performance. Space-charge effects of the electron beam will also be studied via GUN3P simulations [11]. For the unexplained optical spots observed in OTR measurements, a Zemax-based Physical Optics Propagation (POP) simulations will be conducted to evaluate polarization effects. Future considerations will involve studying the response of deflector voltage during scans, and statistical uncertainties that will be quantified using the standard error derived from measurements.

REFERENCES

- [1] W. Blokland and S. M. Cousineau, "A Non-Destructive Profile Monitor for High Intensity Beams", in *Proc. PAC'11*, New York, NY, USA, Sep. 2011, pp. 1438–1442. <https://jacow.org/PAC2011/papers/WE0CN2.pdf>

- [2] *EGH-6210/ EGPS-6210 Electron Source/Power Supply*, Kimball Physics, 2022. https://www.kimballphysics.com/wp-content/uploads/2023/02/EGH-6210_EGPS-6210_2022_1121.pdf
- [3] T. Aitasalo, J. Hölsä, M. Lastusaari, J. Legendziewicz, J. Niittykoski, and F. Pellé, “Delayed luminescence of Ce^{3+} doped Y_2SiO_5 ”, *Opt. Mater.*, vol. 26, no. 2, pp. 107–112, 2004. doi:10.1016/j.optmat.2003.11.006
- [4] R. Thurman-Keup, T. Folan, M. Mwaniki, and S. Sas-Pawlik, “Progress on an Electron Beam Profile Monitor at the Fermilab Main Injector”, in *Proc. IBIC’23*, Saskatoon, Canada, Sep. 2023, pp. 395–399. doi:10.18429/JACoW-IBIC2023-WEP023
- [5] M. W. Mwaniki, P. Snopok, R. Thurman-Keup, and R. Ainsworth, “Measurement techniques using the electron beam profile scanner at the fermilab main injector”, in *Proc. IPAC’25*, Taipei, Taiwan, Jun. 2025, paper WEAN1, to be published.
- [6] J. Bosser, C. Dimopoulou, A. Feschenko, and R. Maccaferri, “Transverse profile monitor using ion probe beams”, *Nucl. Instrum. Methods Phys. Res. A*, vol. 484, no. 1, pp. 1–16, 2002. doi:10.1016/S0168-9002(01)01965-9
- [7] OpenCV, *Open Source Computer Vision Library*, Accessed: 2025-09-02, 2025. <https://opencv.org/>
- [8] Alex Clark and Contributors, *Pillow: PIL Fork*, Accessed: 2025-09-02, 2025. <https://python-pillow.org/>
- [9] ANSYS, *Zemax reference documentation*, Last accessed 19 March 2025, 2025. <https://support.zemax.com/hc/en-us/categories/4403729035667-Reference-Documentation>
- [10] G. Kube, *Imaging with Optical Transition Radiation, Transverse Beam Diagnostics for the XFEL*, TESLA-FEL Report 2008-01, 2008.
- [11] *Gun3P – Static PIC Solver for DC Guns*, Computational Electrodynamics Department, SLAC National Accelerator Laboratory, 2023. <https://confluence.slac.stanford.edu/spaces/AdvComp/pages/240264211/Materials+for+CW23>